Muscular Activity when Walking in a Non-anthropomorphic Wearable Robot

N. L. Tagliamonte[1,*], D. Accoto[1], F. Sergi[2], A. Sudano[1], D. Formica[1], E. Guglielmelli[1]

***Abstract*— Wearable robots should be designed not to alter human physiological motion. Perturbations introduced by a robot can be quantified by measuring EMG activity. This paper presents tests on the LENAR, an intrinsically back-drivable non-anthropomorphic lower limb wearable robot designed to provide hip and knee flexion/extension assistance. In previous works the robot was demonstrated to exhibit low mechanical impedance and to introduce minor alterations to human kinematic patterns during walking. In this paper muscular activity is assessed, demonstrating small alterations in the EMG patterns during the interaction with the robot, in both unpowered and assistive mode.**

I. Introduction

Wearable Robots (WRs) are currently employed for the neuro-rehabilitation of people temporarily affected by walking diseases [1], [2], in structured environments commonly equipped with a treadmill and a body-weight support system, or for the physical assistance of subjects with permanent disorders [3], [4], as an alternative to wheelchairs in daily life scenarios. Representative examples of treadmill-based rehabilitation WRs includes the Lokomat [1], the AutoAmbulator [5], the ALEX (Active Leg EXoskeleton) [6], the PAM-POGO (Pelvic Assist Manipulator - Pneumatically Operated Gait Orthosis) [7] and the LOPES (LOwer-extremity Powered ExoSkeleton) [2]. As an emerging trend, researchers have introduced physical compliance in their designs, for either improved transparency in non-colocated actuation architectures [2], for selectable intrinsic dynamics [8], or for physically modulated impedance through variable impedance actuators [9].

The kinematic structure of the above-mentioned systems is essentially anthropomorphic, *i.e.* it traces the musculoskeletal system, with a direct match among robotic joints and human articulations. Robotic anthropomorphism might cause kinematic incompatibilities due to imperfect alignments among human and robot joint axes of rotation [10], thus resulting in the exchange of unwanted and potentially dangerous interaction forces [11]. Conversely, a non-anthropomorphic structure can exhibit intrinsic robustness against misalignments. Moreover, provided that the design space is not limited by the anthropomorphism constraint, inertial properties and mass distribution can be conveniently optimized in order to minimize mechanical impedance when the robot is backdriven [12]. These principles inspired the design of the LENAR (Lower-Extremity Non-Anthropomorphic Robot), presented in this paper. Indeed, minimizing perturbations to human natural movements is of paramount importance in rehabilitation, when robots are demanded to behave transparently, not to interfere with user's active motion or to intervene with the minimum amount of assistance. This is even more crucial during assessment sessions, when the subject performance has to be evaluated by only using the robot as a measurement device. Recent research addresses the issue of quantifying perturbations to users' motion introduced by WRs. This is usually done by assessing muscular activity during human-robot interaction through surface electromyography (Lokomat [13], LOPES [14], ALEX II [15]). Moreover, different control strategies are often adopted to actively increase robots backdrivability, *e.g.* by resorting to: closed-loop control based on torque feedback from the actuated joints (*zero-torque* approach [14], [15]) or on torques/forces measured at the interface between robot braces and human limbs [16]; active compensation of friction and inertia [17]. Anyhow, active control approaches to increase backdrivability are affected by some issues: *i)* an effective action is only possible within controller bandwidth limits; *ii)* the on-line estimation of required position derivatives introduces noise and delay; *iii)* non-colocation of sensors with respect to actuators can cause instability. On the other hand, intrinsic (*i.e.* at mechanical level) backrivability, can overcome the above-mentioned problems, even though it requires an extra effort in the mechanical design phase. The LENAR was purposively designed to exhibit reduced mechanical impedance by resorting to: *i)* compliant torsion elements in the actuated joints (Series Elastic Actuators, SEAs); *ii)* high efficiency in the gearmotors (to allow retrograde motion) [18]; *iii)* smart distribution of the inertia of the actuation apparatus; *iv)* lightweight design of robotic links.

In a previous work we demonstrated that the robot can be easily backdriven even when unpowered, with minor alterations to lower limb natural joint kinematics and human delivered torques [12]. In the present paper we assessed EMG activity to investigate whether modifications to muscular effort are introduced by the robot and its assistive action.

II. Methods

A. Robotic platform

1) Robot: The LENAR is a treadmill-based device able to assist hip and knee flexion/extension motion through SEAs. As depicted in Fig. 1, the robot kinematic structure significantly deviates from anthropomorphism. For its design,

[1]Università Campus Bio-Medico di Roma, Laboratory of Biomedical Robotics and Biomicrosystems, Center of Integrated Research (CIR), Via Álvaro del Portillo, 21 - 00128 Rome, Italy.

[2]Mechatronics and Haptic Interfaces Laboratory, Department of Mechanical Engineering, Rice University, Houston, TX 77005 and with the department of PM&R, Baylor College of Medicine, Houston, TX 77030.

*Corresponding author: n.tagliamonte at unicampus.it

978-1-4244-7929-0/14/$26.00 ©2014 IEEE

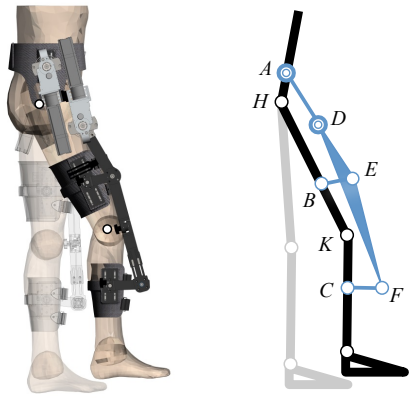

(a) (b)

Fig. 1. (a) 3D drawing of the wearable robot. (b) Schematic representation of the human (gray/black) and robot (light blue) kinematic structures. Points H and K are the hip and knee joints; points A and D are the robot actuated joints (double lines circles); points B, E, C and F are the robot passive joints.

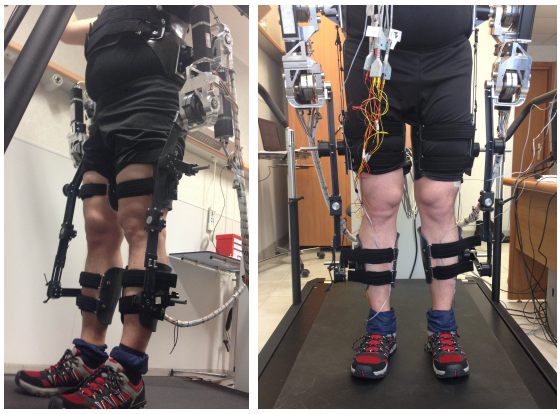

(a) (b)

Fig. 2. Side (a) and frontal (b) pictures of the tester wearing the LENAR.

a systematic search of kinematically compatible planar solutions with 2 DOFs (*topology* level) was pursued [19], while the optimization of a selected topology (*morphology* level) was carried out to minimize actuation torques and forces parallel to the longitudinal axes of body segments, which can potentially damage articulations [20]. The robot comprises one pelvis brace (hosting joint A) and, for each leg, two rotary SEAs [18] actuating joints A and D, one thigh brace (hosting joint B) and one shank brace (hosting joint C). The SEAs (rated power: 300 W, peak torque: 60 N m) were designed to shift the actuator center of mass with respect to the actuated joints. Each gearmotor is proximally located (close to the trunk) thus reducing swinging masses on distal portions. Actuators are intrinsically backdrivable because of the spring and of the high efficiency of the reduction stages (76.5%). Two absolute encoders for each SEA are used to measure the output shaft rotation and the delivered torque. The weight of the robot (about 25 kg) is dynamically balanced by a constant force generator, based on a vacuum cylinder and connected through cables to the pelvis brace.

2) Control hardware: The control hardware consists of four Maxon EPOS2 70/10 units to drive SEA motors and a National Instruments compactRIO-9022 (cRIO), with a FPGA module and an embedded controller running LabVIEW Real Time (RT) software. The cRIO acquires SEA encoder signals (SSI communication, 10 kHz), transmits setpoint values to the EPOS2 units (CAN bus communication, 1 kHz) and runs the high-level controller (200 Hz).

B. Experimental protocol

During the tests, actuated joint rotations and torques were measured. Surface EMG electrodes (DENIS 5026, Spes Medica) were connected to two 4-channel amplifiers (QP522, Grass Technologies). Signals were band-pass filtered (10−1000 Hz) and acquired with the cRIO unit through a NI 9205 16-bit analog input module (sampling frequency: 2 kHz). The activity of five major muscles of the right leg were measured: Rectus Femoris (RF), Vastus Lateralis (VL), Tibialis Anterior (TA), Gastrocnemius Medialis (GM), Biceps Femoris (BF). A tri-axis accelerometer (DE-ACCM3D, Dimension Engineering) was placed on the heel of the subject's right shoe to detect the foot contact with the ground. A voluntary healthy man (24 years old, height 1.78 m, body mass 90 kg) was asked to walk for 1 minute at three walking speeds (0.5, 0.75 and 1.0 m/s) in three conditions:

- Free Walking (FW): The subject did not wear the robot and muscle activity was measured.
- Unpowered Robot (UR): The subject walked wearing the robot with actuators unpowered. Muscular activity was recorded to asses intrinsic transparency of the robot. In this conditions kinematic patterns were also recorded to be used as reference trajectories for the next experimental condition.
- Active Robot (AR): The subject walked wearing the robot controlled to provide assistance based on kinematic patterns pre-recorded in UR mode. Muscular activity was measured to assess robot assistance capability.

Adjustable links and sliders on the braces were regulated to have links BE and CF (Fig. 1) almost perpendicular to the longitudinal axes of the thigh and of the shank. Before the tests, the subject was asked to perform basic hip and knee movements to assess the perceived comfort, then he freely walked at a self-selected speed for 10 minutes (robot unpowered) to get familiar with the device.

In the AR condition PID position control was implemented at the gearmotors level (loop closed by using as feedback signal the rotations before the series springs). With this approach an equilibrium position was set based on the reference trajectory recorded in UR condition, while assistive elastic torques, through physical elasticity ($k = 4.7$ N m/deg), were imparted to the subject. In order to preserve the reliability of the comparison of results from different trials, particular attention was payed during the fixation of the braces of the robot to avoid displacing the EMG electrodes among different tests.

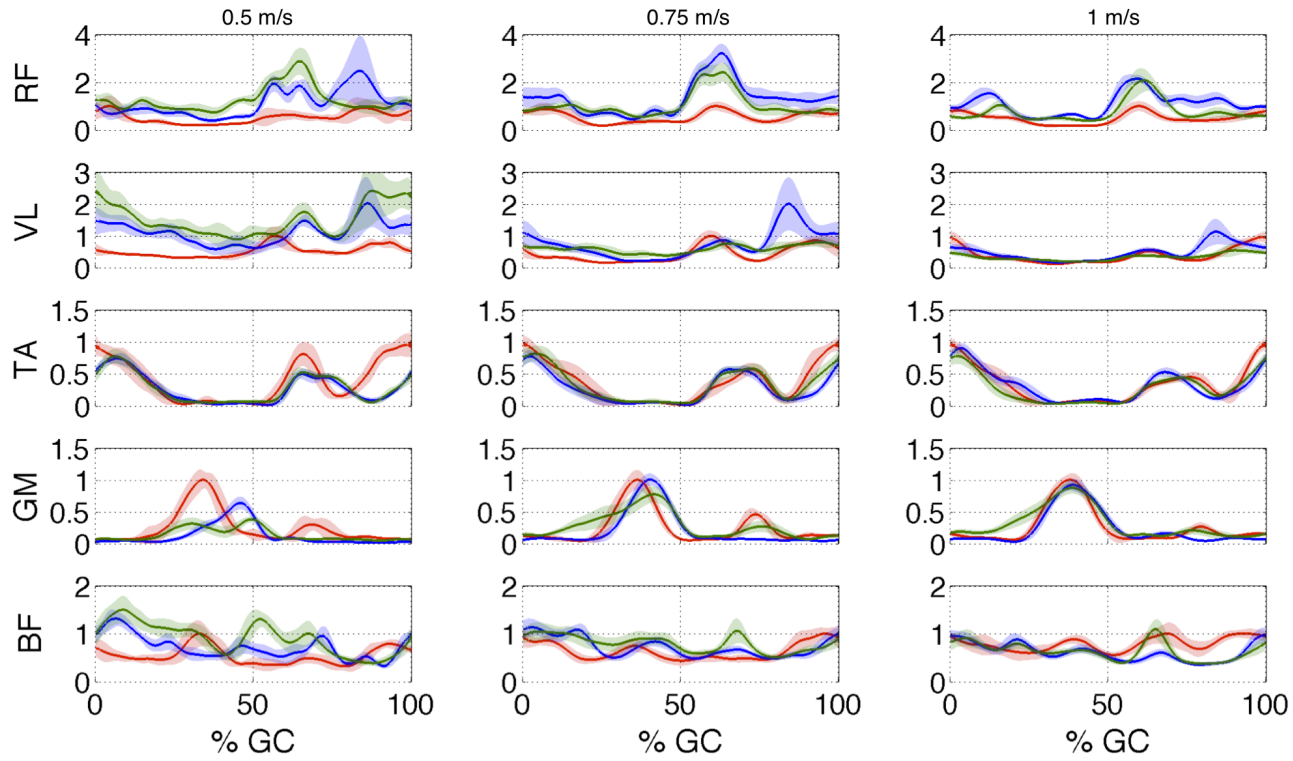

Fig. 3. EMG activity during FW (red), UR (blue) and AR (green) conditions for the three walking speeds. Data are averaged over 30 s for each trial and normalized with respect to the peak of the muscle activity in FW mode. Shaded areas indicate the standard deviation.

C. Data analysis

EMG signals were full-wave rectified and low-pass filtered by using a zero-lag second-order Butterworth filter. A cut-off frequency of 5 Hz was selected similarly to other works, *e.g.* [15]. Accelerometers were used to segment data by identifying heel strike events. To this aim the modulus of the acceleration in the sagittal plane was inspected to extract peaks due to the foot impact. EMG data were averaged over the last 30 s of each test and normalized with respect to the peak of the muscle activity in FW mode. Artifacts were removed by iteratively excluding signals with the highest RMS error, calculated with respect to the mean value, and 20 remaining traces were considered for the analysis. Torques were mapped from the robot joint space into the human joint space by means of the forward kinematics routine presented in [20]. EMG data were compared in the three different conditions, evaluating time patterns and RMS discrepancies.

III. Results

Muscular activity in FW, UR and AR conditions for the three walking speeds are reported in Fig. 3 as a function of the Gait Cycle (GC). RMS values are depicted in Fig. 4. Some alterations in the activation patterns of muscles analyzed in this paper (the major responsible for motion in the sagittal plane) were found for UR and AR conditions, compared to the baseline FW test, which were more pronounced at 0.5 m/s walking speed. Due to the proximal location of the actuators, the activity of distal muscles (TA and GM) was not significantly increased in the conditions entailing the use of the robot (except for the lowest speed). Moreover, the activation of the RF muscle was the one that underwent the most significant variation. The assistance mode decreased the peak measured EMG signal for the GM in the two lowest speeds (no difference in the highest speed). From Fig. 4 it can be noticed that effort distribution (in terms of RMS muscular activation) was reasonably preserved despite the action of the robot. Indeed, the trend of variation (with velocity) of muscle activation was altered in the UR and AR tests with respect to the FW baseline only for RF and TA. The increase of RF and VL EMG signals was likely due to the too high stiffness value used to provide assistance. The range of interaction torques during UR and AR tests at different walking speeds are reported in Table I. The symbols τ_h and τ_k indicate hip and knee torques respectively. It is worth noticing that torques needed to backdrive the robot were similar to the one obtained in other works where active control was indeed used to improve transparency of the robot [16]. Moreover, these values are only in the order of 10% of the torques deliverable by human joints during locomotion. Interaction torques increased with speed because of higher inertial and frictional (in UR condition) effects. Therefore, torques at knee joint were higher with respect to hip torques since robot inertia is localized near the trunk and hence perceived impedance is lower for the (proximal) hip joint.

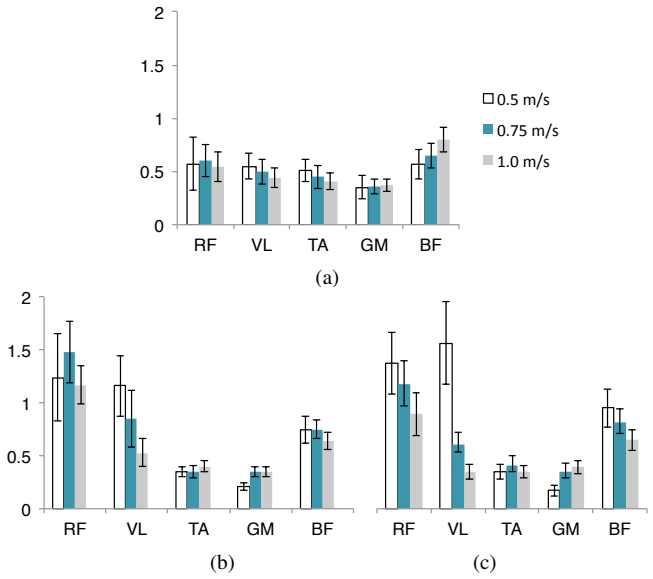

Fig. 4. RMS values of normalized EMG activity for the FW test (a), the UR test (b) and the AR test (c) for the three walking speeds. Bars height indicates the mean of RMS values, while error bars indicate the standard deviation.

TABLE I

PEAK VALUES FOR THE INTERACTION TORQUES DURING UR AND AR TESTS AT DIFFERENT WALKING SPEEDS.

Torque [Nm] (Human joint space)	Walking speed [m/s] 0.5	0.75	1.0
τ_h^{UR}	-1.3÷2.2	-3.0÷4.0	-4.6÷5.7
τ_k^{UR}	-6.1÷5.7	-6.5÷10.0	-8.4÷12.0
τ_h^{AR}	-4.0÷1.5	-5.0÷4.0	-4.0÷4.7
τ_k^{AR}	-3.0÷2.0	-4.1÷3.0	-2.8÷4.2

IV. DISCUSSION AND CONCLUSIONS

EMG activity of major muscles supporting planar motion was assessed on a healthy subject when walking in the LENAR. Despite a re-distribution of muscular effort due to the presence of a worn robotic artifact, as also demonstrated in similar works on other WRs [13], EMG activity was neither highly altered by the assistive action of the robot (even when a simple fixed-stiffness compliant control was implemented) nor by its intrinsic mechanical impedance (robot worn unpowered), at least for some of the analyzed muscles. EMG patterns did not decrease in AR mode with respect to the FW condition (on the contrary they even increased for the RF and the VL muscles) probably because of the use of a simple control algorithm and of the involvement in the test of a healthy subject, who could actively react to the robot. During the experiments the tester did not report discomfort or pain. Peak interaction torques, even in UR mode, were found similar to the ones experienced in other works where active control was purposively employed to improve transparency. Therefore it is expected that implementing zero-torque control in future works will help to further reduce perturbations to human natural motion.

REFERENCES

[1] S. Jezernik, G. Colombo, T. Keller, H. Frueh, and M. Morari, "Robotic orthosis Lokomat: A rehabilitation and research tool," *Neuromodulation: Techn Neur Interf*, vol. 6, no. 2, pp. 108–115, 2003.

[2] J. Veneman, R. Kruidhof, E. Hekman, R. Ekkelenkamp, E. V. Asseldonk, and H. van der Kooij, "Design and evaluation of the LOPES exoskeleton robot for interactive gait rehabilitation," *IEEE Trans Neural Syst Rehabil Eng*, vol. 15, no. 3, pp. 379–386, 2007.

[3] G. Zeilig, H. Weingarden, M. Zwecker, I. Dudkiewicz, A. Bloch, and A. Esquenazi, "Safety and tolerance of the Rewalk exoskeleton suit for ambulation by people with complete spinal cord injury: A pilot study," *J Sp Cord Med*, vol. 35, no. 2, pp. 96–101, 2012.

[4] R. Farris, H. Quintero, and M. Goldfarb, "Preliminary evaluation of a powered lower limb orthosis to aid walking in paraplegic individuals," *IEEE Trans Neural Syst Rehabil Eng*, 2011.

[5] S. Fisher, L. Lucas, and T. A. Thrasher, "Robot-assisted gait training for patients with hemiparesis due to stroke," *Topics in stroke rehab*, vol. 18, no. 3, pp. 269–276, 2011.

[6] S. Banala, S. H. Kim, S. Agrawal, and J. Scholz, "Robot Assisted Gait Training With Active Leg Exoskeleton (ALEX)," *IEEE Trans Neural Syst Rehabil Eng*, vol. 17, no. 1, pp. 2–8, 2009.

[7] D. Aoyagi, W. Ichinose, S. Harkema, D. Reinkensmeyer, and J. Bobrow, "A robot and control algorithm that can synchronously assist in naturalistic motion during body-weight-supported gait training following neurologic injury," *IEEE Trans Neural Syst Rehabil Eng*, vol. 15, pp. 387–400, 2007.

[8] N. C. Karavas, N. G. Tsagarakis, D. G. Caldwell. "Design, modeling and control of a series elastic actuator for an assistive knee exoskeleton," in *Biomed Robot Biomech (BioRob), IEEE/RAS/EMBS Int Conf on*, pp. 1813–1819, 2012.

[9] N. L. Tagliamonte, F. Sergi, D. Accoto, G. Carpino, and E. Guglielmelli, "Double actuation architectures for rendering variable impedance in compliant robots: A review," *Mechatronics*, vol. 22, no. 8, pp. 1187 – 1203, 2012.

[10] A. Schiele and F. C. van der Helm, "Kinematic design to improve ergonomics in human machine interaction," *IEEE Trans Neural Syst Rehabil Eng*, vol. 14, pp. 456–69, Dec. 2006.

[11] N. Jarrass and G. Morel, "Connecting a human limb to an exoskeleton," *IEEE Trans Robot*, vol. 28, pp. 697–709, June 2012.

[12] N. L. Tagliamonte, F. Sergi, G. Carpino, D. Accoto, and E. Guglielmelli, "Human-robot interaction tests on a novel robot for gait assistance," in *Rehab Robot (ICORR), IEEE Intern Conf*, pp. 1–6, June 2013.

[13] J. M. Hidler and A. E. Wall, "Alterations in muscle activation patterns during robotic-assisted walking," *Clin Biomech (Bristol, Avon)*, vol. 20, pp. 184–93, Feb 2005.

[14] E. H. Van Asseldonk, J. F. Veneman, R. Ekkelenkamp, J. H. Buurke, F. C. Van der Helm, and H. van der Kooij, "The effects on kinematics and muscle activity of walking in a robotic gait trainer during zero-force control," *Neural Systems and Rehabilitation Engineering, IEEE Transactions on*, vol. 16, no. 4, pp. 360–370, 2008.

[15] T. Lenzi, M. Carrozza, and S. Agrawal, "Powered hip exoskeletons can reduce the user's hip and ankle muscle activations during walking," *IEEE Trans Neural Syst Rehabil Eng*, vol. 21, pp. 938–948, 2013.

[16] D. Zanotto, T. Lenzi, P. Stegall, and S. Agrawal, "Improving transparency of powered exoskeletons using force/torque sensors on the supporting cuffs," in *Rehab Robot (ICORR), IEEE Intern Conf*, pp. 1–6, 2013.

[17] G. Aguirre-Ollinger, J. E. Colgate, M. A. Peshkin, and A. Goswami, "Design of an active one-degree-of-freedom lower-limb exoskeleton with inertia compensation," *Int J Robot Res*, vol. 30, no. 4, pp. 486–499, 2011.

[18] D. Accoto, G. Carpino, F. Sergi, N. L. Tagliamonte, L. Zollo, and E. Guglielmelli, "Design and characterization of a novel high-power series elastic actuator for a lower limb robotic orthosis," *Int J Adv Robot Syst*, vol. 10, 2013.

[19] F. Sergi, D. Accoto, N. L. Tagliamonte, G. Carpino, and E. Guglielmelli, "A systematic graph-based method for the kinematic synthesis of non-anthropomorphic wearable robots for the lower limbs," *Front Mech Eng*, vol. 6, pp. 61–70, 2011.

[20] F. Sergi, D. Accoto, N. L. Tagliamonte, G. Carpino, S. Galzerano, and E. Guglielmelli, "Kinematic synthesis, optimization and analysis of a non-anthropomorphic 2-DOFs wearable orthosis for gait assistance," in *Int Robot Syst (IROS), IEEE/RSJ Int Conf on*, pp. 4303–4308, 2012.